Title	Sedimentology, sandstone provenance and palaeodrainage on the eastern Rockall Basin margin : evidence from the Pb isotopic composition of detrital K-feldspar
Author(s)	Tyrrell, Shane; Souders, A. Kate; Haughton, P. D. W.; Daly, J. Stephen; Shannon, Patrick M.
Publication Date	2010
Publication information	Vining, B. & Pickering S.C. (eds.). Petroleum Geology : From Mature Basins to New Frontiers : Proceedings of the 7th Petroleum Geology Conference
Publisher	The Geological Society of London
Link to publisher's version	http://dx.doi.org/10.1144/0070937
This item's record/more information	http://hdl.handle.net/10197/3057
DOI	http://dx.doi.org/10.1144/0070937

Sedimentology, sandstone provenance and palaeodrainage on the eastern Rockall Basin margin: evidence from the Pb isotopic composition of detrital K-feldspar.

Shane Tyrrell[1], A. Kate Souders[2], Peter D.W. Haughton[1], J. Stephen Daly[1] and Patrick M. Shannon[1].

[1]Sand Provenance Centre, UCD School of Geological Sciences, University College Dublin, Belfield, Dublin 4, Ireland. Corresponding authors e-mail (shane.tyrrell@ucd.ie)

[2]MicroAnalysis Facility, INCO Innovation Centre and Department of Earth Sciences, Memorial University, St. John's, NL A1B 3X5, Canada

6965 words; 30 references; 1 table; 9 figures

Running Head: Palaeodrainage in the Rockall Basin

Keywords: Sedimentology, palaeodrainage, provenance, Pb isotopes, K-feldspar, Mesozoic, Rockall Basin, Dooish.

Abstract: The Rockall Basin, west of Ireland, is a frontier area for hydrocarbon exploration but currently the age and location of sand fairways through the basin are poorly known. A recently developed provenance approach based on *in-situ* Pb isotopic analysis of single K-feldspar grains by laser ablation multi-collector inductively-coupled mass spectrometry (LA-MC-ICPMS) offers advantages over other provenance techniques, particularly when applied to regional palaeodrainage issues. K-feldspar is a relatively common, usually first-cycle framework mineral in sandstones and its origin is typically linked to that of the quartz grains in arkosic and sub-arkosic rocks. Consequently, in contrast to other techniques, the Pb-in-K-feldspar tool characterises a significant proportion of the framework grains. New Pb isotopic data from K-feldspars in putative Permo-Triassic and Middle Jurassic sandstones in Well 12/2-1z (the Dooish gas condensate discovery) on the eastern margin of the Irish Rockall Basin are reported. These data suggest that three isotopically distinct basement sources supplied the bulk of the K-feldspar in the reservoir sandstones and that the relative contribution of these sources varied through time. Archaean and early Proterozoic rocks (including elements of the Lewisian Complex and its offshore equivalents), to the immediate east, north-east and north of the eastern Rockall Margin, are the likely sources. More distal sourcelands to the north-west cannot be ruled out but there was no significant input from southern sources, such as the Irish Massif. These data, together with previously published regional Pb isotopic data, highlight the important role played by old, near and far-field Archaean – Proterozoic basement highs in contributing sediment to NE Atlantic margin basins. The Irish Massif appears to have acted as a significant, but inert, drainage divide from the Permo-Triassic to the Late Jurassic and hence younger, Avalonian and Variscan, sand sources appear to have been less important on the Irish Atlantic Margin. **(abstract ends).**

Understanding the provenance of sandstones helps in the reconstruction of palaeogeography and in constraining drainage scales and sediment pathways in sedimentary basins. This helps to predict the source and distribution of sandstones, with implications for reservoir quality in the subsurface. However, there are some inherent shortcomings in provenance analysis. Provenance studies are limited by the ability to geochemically distinguish the wide range of potential sourcelands. Additionally, their specific use in the reconstruction of robust palaeodrainage models is problematic, as there are difficulties in recognising and quantifying the extent of sedimentary recycling and mixing (Tyrrell *et al*. in press).

Provenance techniques fall into two broad categories – those that utilise the bulk composition of the sediment or sedimentary rock and those which exploit signals in individual sand grains. Bulk compositional approaches (e.g. petrological techniques, Sm-Nd whole rock) are particularly hampered by problems such as framework grain modification, failure to recognise mixing and recycling, inadequate source characterisation and non-unique signals. These issues cannot be easily overcome with a bulk compositional approach. With the increased availability of *in-situ* micro-analytical techniques, provenance studies increasingly utilise geochemical or isotopic signals in single grains of a specific mineral (e.g. Cawood *et al.* 2004; Clift *et al.* 2008). However, although these techniques enable sourcelands to be distinguished, the full transport history experienced by individual framework components often remains unconstrained. Many provenance tools use 'trace' components that may be difficult to relate to the framework grains that determine reservoir characteristics. Robust mineral phases (e.g. zircon) may have been recycled through one or more intermediary sediments or sedimentary rock. In contrast, unstable mineral grains (e.g. K-feldspar) are less likely to survive sedimentary recycling, and, therefore, if present, can be regarded as first-cycle components derived directly from source. The identification of first cycle detritus is key to resolving drainage scales and sediment transport pathways in reservoir sandstone intervals. Recent studies have demonstrated the utility of the Pb isotopic composition of detrital K-feldspar as a sand provenance tool that can be applied on a regional scale (Tyrrell *et al.* 2006, 2007; Clift *et al.* 2008). As detrital K-feldspar is unlikely to survive more than one sedimentary cycle, grains can be tracked back directly to their basement source.

In recent years Pb K-feldspar data have been collected from NW European Margin basins as part of an ongoing study of Permo-Triassic to Lower Cretaceous sediment dispersal (Tyrrell *et al.* 2007, in press). The aims of this regional work are to understand better the large-scale controls on drainage development throughout the Mesozoic, to examine the evolving drainage patterns prior to and during the break-up of Pangaea, to identify potential linkages between basins on the conjugate Atlantic margins, and to consider the implications for regional sand distribution within and across the lightly explored basins west of Ireland.

Detailed investigations of the c.6km of Mesozoic and Cenozoic stratigraphy in the Rockall Basin have been hampered by the lack of wells drilled in the basin. Until recently, stratigraphic control points were limited to a single DSDP borehole (610) in the southwest of the basin, which penetrated Miocene and younger sediments, and a small number of boreholes in the NE Rockall Basin within the UK sector. However, a programme of shallow borehole drilling carried out in 1999 (Haughton *et al.* 2005) allowed the Mesozoic stratigraphy of the eastern basin margin to be directly constrained for the first time. The oldest definitively dated rocks penetrated by these boreholes are Late Jurassic (Early Kimmeridgian). More recently, exploration drilling on the eastern Rockall Basin margin, offshore NW Ireland (well 12/2-1 and sidetrack 12/2-1z; Figure 1), led to the Dooish gas condensate discovery which is hosted in sandstones of Permo-Triassic and Middle Jurassic age (see below). The cores from well 12/2-1z present a unique opportunity to expand our knowledge of evolving drainage in the region. In this paper, new provenance data obtained from both the Permo-Triassic and Middle Jurassic reservoir sandstone intervals in this well are discussed in detail. In addition, these data are incorporated with recently published data from Triassic, Upper Jurassic and Cretaceous sandstones from the Slyne, Porcupine and eastern Rockall basins respectively in order to understand better regional sediment dispersal patterns and controls on palaeodrainage development. These impact directly on the prospectivity of the Irish Atlantic margin basins.

THE PB IN K-FELDSPAR PROVENANCE TOOL: RATIONALE AND APPROACH

The Pb-in-K-feldspar provenance tool can provide valuable information on regional sand dispersal in sedimentary basins, especially, as in this case, where the reservoir intervals are feldspathic. The Common Pb isotopic signature of K-feldspar has proved to be a powerful method of mapping gross crustal structure (e.g. Connelly & Thrane 2005) and hence potential sand source areas. Systematic regional variations in common Pb composition are seen at sub-orogenic scale (<100 km) in both active mountain belts and ancient orogens (Vitrac *et al.* 1981) reflecting the assembly of basement domains with different ages and U-Th-Pb fractionation histories. Therefore, broad regional patterns in Pb composition can be identified by characterizing a relatively small number of granite feldspars (De Wolf & Mezger 1994, Connolly & Thrane 2005). K-feldspar typically contains between 5 and 150 ppm Pb,

and has low U and Th contents (typically <1ppm), and hence the corrections to the common Pb signature for radioactive decay are negligible.

K-feldspar is a common mineral in many sandstones and a key constituent of arkose, and it has been shown that detrital grains retain the Pb isotopic signature of their source (Tyrrell *et al.* 2006). Importantly, the source of K-feldspar is very likely linked to the source of the majority of the quartz grains. Therefore determining K-feldspar provenance ultimately can constrain the source of the majority of the framework grains.   With the advent of *in-situ* techniques (laser-ablation inductively-coupled plasma mass spectrometry (LA-ICPMS) and secondary ion mass spectrometry (SIMS)) it is now possible to measure variations in the Pb composition within individual K-feldspar sand grains so that the extent of intra-grain variation and mixing of different grain populations can be isolated (Tyrrell *et al.* 2006). The rapid, non-destructive, *in-situ* analysis of large numbers of individual grains by LA-MC-ICPMS within an arkose represents a significant advance in provenance characterisation (Tyrrell *et al.* 2006, 2007). The use of ion counter instead of Faraday collectors (see below) allows for the analysis of low Pb and finer grain sizes (Tyrrell *et al.* in press).

Five principal Pb basement source domains have been distinguished in the North Atlantic region using published Pb data (Figure 1; Tyrrell *et al.* 2007 and references therein). Spatially, these zones strike NE-SW and correspond to the basement terranes involved in the assembly of Laurentia and Rodinia, the Caledonian collision of Laurentia with Avalonia, and the Variscan Orogen. Although there are variations within each of these zones, there is a broad shift towards more radiogenic Pb values towards the SE reflecting the history of crustal growth. Pb domain 1 comprises Archaean and Palaeoproterozoic basement and has the least radiogenic Pb. Pb domain 2 corresponds mainly to older basement reworked during late Meso- and Palaeoproterozoic. Pb domain 3 largely comprises Mesoproterozoic basement with Neoproterozoic metasedimentary rocks and younger Caledonian granites. Pb domain 4a corresponds to Avalonian basement and has a large overlap with Pb domain 4b, which corresponds with the Variscan and contains radiogenic Pb remobilised from Avalonian basement during end-Palaeozoic closure of the Rheic Ocean.

MESOZOIC SEDIMENT DISPERSAL INTO NE ATLANTIC MARGIN BASINS:

During the Permian and Triassic, northwest Europe lay at low latitudes close to the margins of the Pangaean Supercontinent. Late Permian and Early Triassic sedimentary basins in the region are characterised by non-marine deposits, comprising local alluvial fans, extensive fluvial deposits, playa lakes and aeolian sands in successions in excess of 1 km thick (Warrington & Ivimey-Cooke 1992). The early Triassic sandstones form reservoirs for hydrocarbons offshore west of Ireland (the Corrib gasfield in the Slyne Basin), in the East Irish Sea Basin (the Morecombe gasfield), in the Wessex Basin of southern England (the Wytch Farm oilfield) and in the North Sea. The Lower Triassic sandy deposits (Sherwood Sandstone and equivalents) are overlain by the Middle-Upper Triassic dominantly mud-prone (but locally sand-rich) successions (Mercia Mudstone). The 'Budleighensis' palaeo-river system drained northward from the Variscan Uplands into the Wessex Basin (Audley-Charles 1970) and extended further north into the Cheshire Basin, and probably as far as the East Irish Sea Basin. However, though, until recently, the extent of drainage systems with this geometry in basins further north and west remained unclear.

In the Slyne Basin west of Ireland (Figure 1), Sherwood sandstone equivalent Triassic sandstones host the Corrib gasfield and comprise fine- to medium-grained arkosic fluvial and alluvial sandstones with sub-ordinate sand-flat and playa mudstone deposits (Dancer *et al.* 2005). Previous palaeodrainage models for these sandstones, based on borehole dipmeter logs and whole-rock geochemistry, suggested derivation from the south and south-west (the Variscides) with some input from the uplifted Irish mainland (Dancer *et al.* 2005). Recently published Pb isotopic data for the K-feldspar component suggest a contrasting interpretation; two distinct Pb populations appear to have been sourced from Archaean and Proterozoic crust, suggesting derivation from a potentially wide area to the north and west (Tyrrell *et al.* 2007). Significantly, grains appear to have been dispersed across the subsequent site of the Rockall Basin, with drainage scales likely to have been in excess of 500 km. These data indicate that very few (if any) grains could have been derived from the Irish Massif or, significantly, from the Variscan Uplands. Furthermore, in basins west of Shetland, new Pb K-feldspar data (Tyrrell *et al.* in press) from Middle-Upper Triassic Foula Formation sandstones (Strathmore Field) indicate local

derivation from Archaean – Palaeoproterozoic rocks on the margins of the rift basin (Nassugtoqidian Mobile Belt of East Greenland and/or the Lewisian Complex of NW Scotland), though an eastern or western source cannot be distinguished. Here, the Pb K-feldspar data is in broad agreement with U-Pb detrital zircon geochronology (Morton *et al.* 2007). Regionally, data from Triassic sandstones suggest that sediment dispersal was at this time controlled by uplifted Archaean and Proterozoic basement, with the Irish Massif acting as a drainage divide for south-derived Variscan sediment.

The Porcupine Basin, southwest of the Slyne Basin (Figure 1), includes a Jurassic sequence deposited during a phase of rifting (Croker & Shannon 1987; Naylor & Shannon, 2005). In the northern part of the basin, an Upper Jurassic (Kimmeridgian-Tithonian) sequence of low-energy fluvial (meandering river) and marginal marine facies is present. These sandstones are the reservoirs for the Connemara oil accumulation in well 26/28-1 (Figure 1). These facies are replaced southwards by marine sandstones and deep-water fans (Butterworth *et al.* 1999; Williams *et al.* 1999), which host the Spanish Point gas condensate discovery (35/8-2). Previous work (Butterworth *et al.* 1999) suggested north to south basin-axial flowing drainage in the Upper Jurassic section in the Northern Porcupine Basin. Published Pb data from K-feldspars from the Upper Jurassic of the Northern Porcupine basin (Tyrrell *et al.* 2007) define two Pb isotopic populations. Both occur in sandstones from wells 26/28-1 and 35/8-2. These data have been interpreted (Tyrrell *et al.* 2007) to represent axial derivation from a northern source, likely from the uplifted Porcupine High, with possible transverse input from the basin margins. Dispersal distances are envisaged as being c. 100 km. These data also indicate that the sandstones in quadrants 26 and 35 share the same source and that the northern fluvial systems may have been linked with the turbiditic fans further south. Grains derived from Archaean and Palaeoproterozoic sources are very rare in this dataset, suggesting drainage did not extend across the developing Rockall Basin at this time.

Previously published Pb data from detrital K-feldspar grains from Cretaceous sands and sandstones sampled from the western flanks of the Porcupine Bank (eastern Rockall Basin margins; 83/20-sb01 and 16/28-sb01; Figure 1) show relatively radiogenic compositions. These sediments, sampled from shallow boreholes, are calcareous and appear to have been deposited in a high-energy shelf environment (Haughton *et al.* 2005). The sedimentology of these sands and the Pb isotopic

composition of the K-feldspar component suggest they are locally derived directly from the Porcupine

High (Tyrrell *et al.* 2007). Transport of K-feldspar sand grains across the Rockall Basin is not indicated.

THE DOOISH GAS CONDENSATE DISCOVERY, EASTERN ROCKALL BASIN:

The Dooish gas condensate discovery, on the eastern margins of the Rockall Basin, comprises pre-rift

sandstones in a 40 km^2 tilted fault block sealed by post-rift sediments of Late Cretaceous age (Figure

2). Well 12/2-1, some 125 km northwest of Donegal, was drilled in 2002 in order to test the prospect.

The target sandstones were presumed to be Middle-Late Jurassic in age, based on jump seismic

correlation with the Slyne - Erris Basin to the south, though it was recognised that they could be as old

as Permo-Triassic. Well 12/2-1 successfully demonstrated the presence of a working petroleum system

in the eastern Rockall Basin, but insufficient biostratigraphic information was retrieved to date precisely

the reservoir intervals. Well 12/2-1z, a deviated sidetrack of 12/2-1, was drilled in 2003 in order to

determine the vertical extent of the hydrocarbon column penetrated by the earlier well and to

investigate the potential of the previously undrilled deeper section.

Well 12/2-1z terminated in Late Carboniferous interbedded sandstones and shales at a depth of c.4.5

km (Figure 3). Gas condensate was recorded within younger sand-prone intervals that span ages

between Permian and Lower Cretaceous (see below). A total of 3 cores were retrieved from the well.

This study utilises new sedimentological logging of the cored intervals, together with well reports and

completion logs to constrain depositional and stratigraphic context for the provenance analysis.

METHODOLOGY:

Core logging and sampling:

The 3 cored intervals in well 12/2-1z, comprising a total of 90 metres of section, were logged at a scale

of 1:50. The cores were sampled at intervals of c.2 metres, with sand-rich beds and distinct facies

intervals preferentially targeted. Wherever possible, core plug trims were used in preference to

sampling the core directly. Thin sections of these samples were prepared, and their petrography

assessed optically. On the basis of bulk facies and petrographic assessment, a subset of samples was selected for provenance analysis (see below).

Provenance Analysis:

Imaging and EMPA analysis: Thin sections of c.300 µm thickness were prepared from which K-feldspar grains were imaged using backscatter electron (BSE) and cathodoluminescence (CL) at the Electron Microprobe Laboratory, Geowissenschaftliches Zentrum, Göttingen, Germany. The majority of the imaged grains were analysed using electron microprobe analysis at the above facility, to constrain bulk composition of the feldspar grains.

Pb analysis: The analytical techniques used are detailed in Tyrrell *et al*., in press. Data were acquired using a Neptune MC-ICPMS linked to a Geolas 193 nm Excimer laser, at the Microanalysis Facility, InCo Innovation Centre, Memorial University, Newfoundland (MUN). Initially, a Faraday cup array was used to collect the isotopic data. However, grains with low Pb concentration (<30 ppm) produced weak Pb ion beams, resulting in unacceptably poor errors (2SE >1%) in Pb isotopic ratios. More recently, the technique has been refined such that reliable Pb isotopic measurements can be made on grains smaller than 50µm long axis or with low (<10 ppm) Pb concentrations. This advancement utilises ion counters, in preference to Faraday cups, for more accurate measurement of weak Pb ion beams. This technique requires *in-situ* measurement of the Pb concentration in the K-feldspar grains prior to isotopic analysis. This enables the laser spot size to be adjusted during isotopic analysis such that sufficient, but not excessive, Pb is released. Optimising the Pb ion beam allows for the reduction of analytical error and prevents damage to the ion counter array which can result from strong beams. Pb concentrations were measured using an Element ICPMS in the Microanalysis Facility at MUN. U and Th concentration of individual K-feldspars, used to constrain potential radiogenic growth, were measured at the same time (Table 1).

In the case of all the analytical approaches, the data can be acquired rapidly and require only a previously-imaged, thick (c.300 µm) polished thin section, thereby retaining the grain context within the sedimentary rock sample. The approach also uses minimal core material and can be undertaken on

9

smallcore chips or plug trims. Previous workers have used multiple- single-grain leaching techniques coupled with TIMS analysis (Hemming *et al.* 1996), but this approach does not allow for potential intra-grain heterogeneities to be characterised prior to and avoided during analysis. The use of ion microprobe techniques (Clift *et al.* 2001; 2008) allow for *in-situ* high spatial resolution analysis (c.20μm spot sizes), but produce consistently larger errors on ^{204}Pb dependent ratios than LA-MC-ICPMS analysis. In previous LA-MC-ICPMS Pb K-feldspar work (Tyrrell *et al.* 2006, 2007) data could only be retrieved from grains larger than c.300 μm long axis, but the refinement of the technique has allowed for Pb analysis of very fine-grained sand and even silt grains - with similar levels of spatial resolution to those in ion microprobe analysis now possible (c.20 μm laser spot sizes). Analytical uncertainties (2SE on ^{206}Pb/^{204}Pb) are typically <0.5% for the Faraday configuration and typically <0.25% with the ion counter collection array. In all cases, ^{204}Pb, ^{206}Pb, ^{207}Pb and ^{208}Pb were measured. ^{202}Hg was also measured during analysis in order to correct for isobaric interference of ^{204}Hg on ^{204}Pb. Standard-sample bracketing, using NIST standard glass 612 (^{206}Pb/^{204}Pb = 17.099), was carried out in order to correct for mass bias fractionation (Tyrrell *et al.* in press).

RESULTS:

Well stratigraphy:

Wireline logs from 12/2-1z were used to constrain the well stratigraphy. On the basis of gamma and sonic velocity response, three post Carboniferous sand-prone packages have been identified and targeted for further investigation (Figure 3). These form a continuous sand-rich sequence which hosts the hydrocarbon column. The oldest of the three intervals, referred to here as the A sandstones, is c.225 m thick and shows typically low gamma response in sandstones, intercalated with thin high gamma mudstones. The A sandstones are overlain directly by the B sandstones (c. 128 m thick). The boundary is marked by a distinct change in the character of the gamma log profile (Figure 3), with much lower variations, but with an overall higher gamma response within the sandstones. This change is attributed to an increase in K-feldspar modal abundance. The C sandstones are very thin (c.4.5 m) and directly overlie the B sandstones. The C sandstones have a similar low gamma response to the A sandstones.

The deepest core (core 3), from 4098 to 4078 m drillers depth (d.d.) RKB, comprises a 20m interval of well-sorted, medium-coarse grained, red-buff sandstones with minor mudstones, and includes the boundary between the A and B sandstones (Figure 3). Cores 1 and 2 represent a near-continuous c.70 m section some 57 m above the top of core 3 (4021.1 to 3952 m d.d.RKB). These cores, corresponding to the uppermost part of the B sandstones and the entire C sandstone, comprise coarse pebbly- to fine-grained sandstones, calcareous sandstones, siltstones and minor mudstones, with a distinctive volcanic horizon toward the top of the core 1.

Given the unfossiliferous nature of the cored intervals, their age has yet to be firmly established. Biostratigraphical results from released well reports suggest an early Permian (Asselian) age for the lowermost, uncored part of the A sandstones and a Middle Jurassic to Earliest Cretaceous age for the B and C sandstones. In the absence of definitive biostratigraphic data, released well reports have assigned a broad Permo-Triassic age for the uppermost and cored part of A sandstones, and B and C sandstones are assigned a tentative Middle Jurassic age. For the purposes of this study, the important issues are the compositional variations between packages and the broad correspondence between this well and others in the region at the level of Permo-Triassic versus Jurassic-Cretaceous.

Core description:
The short section of cored A sandstones (c.4.5 m) comprises well sorted medium to coarse grained buff coloured sandstones with subordinate siltstones and mudstones (Figure 4). The sandstones are characterised by common low-angle cross-stratification and minor ripple cross-lamination. The top of the package is marked by muddier horizons, with a distinctive red mudstone bed just beneath the contact with the A package. The boundary between the A and B sandstones occurs as an erosion surface at 4092.5 m d.d.RKB. This is directly overlain by a pebbly-based, medium-grained buff-coloured sandstone. B sandstones in core 3 are distinguished from the underlying A sandstones by their more abundant coarser sandstones beds, frequently with distinct erosive bases and mud rip-up clasts. The gamma log confirms an abrupt change in character at the A/B contact.

B sandstones in core 2 comprise coarse to pebbly sandstones (Figure 4) in graded beds with common erosive bases. They tend to be cross-stratified, particularly towards bed tops (Figure 4). The sandstones contain extraclasts (pebbles of vein quartz, granite and granitic gneiss) and rounded fragments of intraclastic calcareous sandstones. Sandstone beds frequently appear to have been internally remobilised or disrupted during deposition, and there are abundant post-depositional siderite-cemented fractures. Coarser beds become less abundant at higher levels (above c.3991 m d.d. RKB, toward the top of core 1 and base core 2), where there are abundant calcareous bands, marls and siltstone beds. Here, the logged interval is marked by a change from buff to dominantly grey colour. There are several distinct coarsening-upward beds (0.5 - 1 m scale) which comprise mud dominated bases with sandy lenses, becoming increasingly sandy toward their tops which contain mud-lenses (e.g. at depth 3976.5 – 3975.5 m). These heterolithic beds are frequently associated with *in-situ* calcareous horizons.

The boundary between the B and C sandstones occurs toward the top of core 1 (3968 m d.d. RKB) and appears conformable. It is marked by a distinct, green, pebble-based sandstone bed overlying B package muddy siltstones. The C sandstones are c. 4.5 m thick and comprises coarse to medium grained, sandstones with distinct cm-scale pebble-rich bands. There are abundant buff, rounded, intraclastic calcareous sandstone fragments (Figure 4) which appear to be enveloped by green remobilised sandstones. The green colour is attributed to the presence pf fine grained glauconite. The top of the C sandstone (3963.5 m d.d.RKB) is marked by a dark green, vesicular, volcanic rock.

Depositional environments:

A sandstones: In cored A sandstones, the sedimentary structures, the well-sorted nature of the sandstones, lack of marine indicators (e.g. fossils, glauconite) and the presence of rounded grain-types are suggestive of a non-marine aeolian or fluvially-reworked aeolian facies with possible fluvial unconfined channel ('sheet') sandstones.

B sandstones: The coarse nature of the B sandstones in core 3 and the presence of both trough cross-bedding and low-angle cross-stratification suggest intermittent fluvial shallow channel sandstones and sandflat deposition. The calcareous layers are interpreted as calcretes, indicating a semi-arid environment. The remobilised or disrupted appearance of some beds may be due to modification during pedogenesis.

The coarse sandstone packages toward the base of core 2 are interpreted to be the deposits of relatively a high-energy alluvial/fluvial system, with channel lag deposits and sandy bar-forms interbedded with unconfined sheet sand deposits. The energy of this system wanes upward with more frequent unconfined sheet sand deposits, lower energy channels, and abundant mudstone-lenses.

The finer-grained, grey, muddy lithologies observed from the upper part of core 2 appear likely to represent overbank deposits. Calcareous horizons are interpreted as palaeosols, and occur as *in-situ* continuous mature calcrete horizons, *in situ* nodules (immature calcretes) and possibly reworked intraformational clasts. Disruption of lamination is likely attributed to soil formation processes. The heterolithic beds in core 1 and 2 suggest a tidal influence. The structures in the upper part of core 2 and lower part of core 1 are indicative of the transition from a low-energy floodplain/lacustrine to an estuarine environment with possible tidal influence.

C sandstones: The presence of glauconite in C package sandstones suggests a marine environment, possibly a shoreface setting (Figure 4). The disrupted appearance of C package sandstones may be caused by de-watering and/or related to deposition on an unstable slope. The volcanic horizon occurring above package C is interpreted as a lava flow as its upper boundary appears blocky and weathered.

Sandstone Petrography

A sandstones: Sampled sandstones are well-sorted sub-arkosic arenites, with sub-angular to rounded grain shapes (Figure 5A). Rounded grains may represent an aeolian grain population which has been reworked by fluvial action. K-feldspar is common (c.15% modal abundance), and it has a very fresh

appearance, commonly displaying perthitic textures (Figure 5D). Traces of plagioclase, muscovite mica and detrital clay occur. Minor lithic fragments, dominantly of plutonic igneous origin, also occur. Macroporosities vary between 5 and 15%.

B sandstones: Sampled sandstones are generally texturally more immature than A sandstones and are lithic arkoses. They comprise abundant K-feldspar (up to c.30%) with a significantly higher lithic component than A sandstones. Lithic fragments are dominantly quartzo-feldspathic aggregates of likely plutonic igneous origin, but also including minor gneissic (Figure 5E) and schistose fragments. Some fine-grained B sandstones are calcareous and contain micritic intraclasts (Figure 5F). Trace accessory minerals include albite, muscovite mica and detrital clay. Macroporosities in these sandstones ranges between 5 and 20%. Calcite occurs as a patchy pokilotopic pore-filling cement in all the sandstones. Minor authigenic illitic clays occur, usually as a grain-rimming cement, and pyrite is present as a late phase.

C sandstones: Sampled sandstones are relatively well sorted and invariably display a bimodal grain size distribution comprising a fine angular grain component and a medium-coarse rounded grain component (Figure 5C). The sandstones are arkosic, with K-feldspar dominant, and sublithic, with plutonic igneous fragments most common. The sandstones contain glauconite. Macroporosity is less than c.15%.

Analytical results:

Sixty seven Pb isotopic analyses of sixty four K-feldspar grains/crystals from sandstone intervals in well 12/2-1z K-feldspar were carried out and the data are presented in Table 1. Of these, 18 were obtained using a faraday collector configuration with the remaining analysis carried out using the ion counter collector configuration (see above).

Seven grains were analysed from two samples of the A sandstones in core 3, 17 grains from six samples of B package sandstones in core 3, 21 grains from seven samples of B sandstones from cores 1 and 2, and 19 grains from 3 samples of C sandstones from core 1. The bulk composition of 45

of these grains was constrained using electron microprobe analysis. Results show that feldspars are dominantly orthoclase, with an average composition of Or : Ab : An = 96.08 : 3.83 : 0.08. There appears to be no link between the Pb isotopic and the bulk feldspar composition.

Overall, the feldspars largely exhibit relatively unradiogenic Pb isotopic compositions, with ^{206}Pb/^{204}Pb ratios varying between 13.53 and 16.70, averaging at 14.92, with only three more radiogenic grains with ^{206}Pb/^{204}Pb in excess of 17. Overall, the Pb data form three distinct groupings or trends. These groupings are considered to represent three distinct sources, though it should be noted that, geographically different sources may have a shared basement history and thus have the same Pb isotopic composition. Source 1 corresponds to a grouping of the most unradiogenic Pb compositions plotting within Pb domain 1 (see above); Source 2 corresponds to a group of data with an apparent linear trend, while Source 3 forms a tight grouping of grains, more radiogenic than Source 1, and plotting within Pb domain 2 (Figure 6).

Samples 9 and 10 from B package sandstones in Core 3 are granitic clasts from which several K-feldspar crystals were analysed. Pb isotopic analyses of 3 K-feldspar crystals from sample 9 exhibit an unradiogenic composition plotting within a restricted range (Figure 6), but isotopic analyses of 4 K-feldspars from sample 10 show a significant spread in ^{207}Pb/^{204}Pb. This illustrates that K-feldspars from the same source rock can, at least in terms of the ^{207}Pb, can have a range of Pb isotopic compositions. This characteristic could help explain some of the outlying Pb isotopic compositions, and could be due to small initial variations in Pb, U and Th, either between K-feldspars in the same rock or within individual zoned crystals. However, the differences appear insignificant in terms of the regional variation in Pb, for example, despite the Pb isotopic variation in sample 10, all data vary little in terms of ^{206}Pb/^{204}Pb and plot along a steep trend line.

PROVENANCE INTERPRETATION:

The majority of K-feldspars from A sandstones show a Pb isotopic composition that falls within the range defined by Source 2. There is a relatively minor component (2 grains) which fall within Source 1

(Figure 3). K-feldspars from lower B sandstones (i.e. those from core 3) show bimodal Pb isotopic populations, attributed to Source 1 and 3, but with no Source 2 grains (Figure 3). K-feldspars from upper B sandstones (i.e. those from cores 1 and 2) also have a bimodal Pb isotopic composition, corresponding to Source 1 and 2, but with no Source 3 grains. K-feldspars from C sandstones plot within Source 1 and 3, with no Source 2 grains, a similar distribution pattern to that seen in lower B sandstones (Figure 3).

In order to constrain the sourcelands, the three "source" ranges have been plotted with Pb isotopic data for basement in the region (Figure 7). There is good correspondence between source 1 and elements of the Lewisian Complex, in particular the offshore Stanton Banks area, but grains with this composition could also have been derived from elements of the Nagssugtoqidian of SE Greenland. Source 2 appears to correspond with the linear data arrays that are manifest in some of the blocks within the Lewisian Complex (e.g. Uist Block).

Source 3 has a more radiogenic Pb composition than source 1, but a less radiogenic composition to other sampled regional basement units (e.g. the Rhinns Complex) and offshore highs (e.g. Rockall Bank, Porcupine High). Reconstructions of the North Atlantic region suggest continuation of orogenic belts across the Atlantic (Tyrrell *et al.* 2007), yet much of the offshore basement remains poorly characterised. Source 3 may correspond to an area of as yet unsampled basement in the region. On the basis of its Pb isotopic composition, this source seems unlikely have an affinity with the oldest basement in the region (Lewisian, Nagssugtoqidian), but could feasibly represent basement of Ketilidian affinity. Ketilidian-affinity crust in the region is likely to display a broader range in Pb isotopic composition than that shown by the limited samples analysed from the Rockall Bank. Such a source could have been available at times during deposition of the Dooish sandstones, but may presently be buried. Naturally, there are problems speculating on the past geographical occurrence and areal extent of such basement but, given its Pb isotopic composition (plotting in the Pb domain 2) it could occur to the immediate east of the Dooish area, or alternatively, within the northern Rockall Bank.

Palaeogeographic reconstructions for the intervals of deposition of the Dooish sandstones and the position of likely sources areas are shown in Figure 8. A sandstones have likely been derived directly from the north or from the north-west, with drainage scales in the order of 300 km envisaged. More local sources, directly from the east, north-east and north are suggested for the lower B sandstones. Data from upper B sandstones suggest dominantly north and north-east derivation, while C package sandstones could have been derived from more local sources to the north, north-east and east.

There is an abrupt change in source area between A sandstones and overlying lower B sandstones as sampled from core 3, manifesting as a switching off of Source 2 and an influx on Source 1 and 3 grains. This change of source area corresponds with an abrupt change in the wireline character at the boundary of these units, and is consistent with the apparent prolonged period of non-deposition between the Permo-Triassic and Middle Jurassic. During this hiatus it is possible the palaeo-erosion surface and hinterland geological composition changed considerably.

Upper B sandstones (from cores 1 and 2) have a different provenance character to the lower B sandstones (core 3), with the loss of Source 3 grains in the upper B sandstones and the presence of a Source 2 population, while Source 1 continues to be important. This may reflect a more gradual evolution of drainage/erosion in the hinterland than that suggested by the abrupt change between the A and B sandstones. However, analysis of the intervening B sandstones between the top of core 3 and base of core 2 is required in order to test this hypothesis.

Another rapid change in sourcing occurs between the deposition of B and C sandstones, with the disappearance of Source 2 grains and a bimodal distribution of distinct Source 1 and 3 grains. This change could be linked with the change in depositional environment, with marine currents influencing the routing of grains and the detrital composition of the sandstones.

It is important to note that in bulk terms, Source 1 appears to have been consistently available as a source during the Permo-Triassic and Middle Jurassic. Also, at every sampled stratigraphic level, either Source 2 or 3 is available, but never at the same time. The intermittent delivery to the basin of either

17

Source 2 or 3 grains could be caused by the periodic rejuvenation of specific tributary systems, possibly linked to variations in uplift rates in the hinterland, or may be the affect of subtle climatic factors affecting the delivery of grains to the basin. The variation of provenance with stratigraphy in the succession highlights the potential of the Pb-in-K-feldspar provenance technique as a tool in the correlation of sand-prone but unfossiliferous intervals.

IMPLICATIONS FOR REGIONAL SAND-SOURCING:

The three source-types can be compared with Pb isotopic data from K-feldspar grains in 1) Triassic sandstones from Corrib gasfield sandstones in the Slyne Basin; 2) Upper Jurassic sandstones from the Northern Porcupine Basin; and 3) Cretaceous sandstones from the western margin of the Porcupine Bank (Figure 9).

Source 1 and 3 show strong correspondence with the two groupings observed in Corrib gasfield sandstones. This suggests that Triassic Corrib sandstones share the same provenance as the lower B sandstones and the C sandstones, but have a different provenance to A sandstones in the Dooish area of the Rockall Basin. It is envisaged that grains from the Corrib gasfield sandstones were transported across the nascent Rockall Basin (Tyrrell *et al.*, 2007; Figure 8), but more local sourcing within or close to the Slyne Basin could as yet be unrecognised. Though drainage length scales appear to be shorter in the Permo-Triassic of the eastern Rockall basin, the orientations are similar to those interpreted for the Triassic of the Slyne Basin.

There is no correspondence between the three Dooish source-types and detrital K-feldspar data from Upper Jurassic sandstones in the Northern Porcupine Basin, or from Cretaceous sandstones on the margins of the Porcupine Bank. This suggests that Jurassic sandstones deposited to the north and to the south of the Porcupine High have a contrasting provenance, and that the Porcupine High itself could have been uplifted and acted as a barrier to drainage during the Middle to Late Jurassic (Figure 8). It appears that local sand sourcing dominated during the Middle and Late Jurassic in both the Rockall and Porcupine basins, with drainage scales in both basins interpreted to be c.100km.

18

Additionally, In the Upper Jurassic of the Porcupine Basin, recycled Carboniferous sedimentary rocks are suggested to have been an important source (Robinson and Canham, 2001). These seem to play a far less important role in the Dooish sandstones, where petrography clearly shows crystalline plutonic igneous and metamorphic basement as the predominant source.

In overall terms, the pattern of detrital Pb isotopic compositions of K-feldspars in Permo-Triassic to Cretaceous sandstones in basins on the NW European margins highlights the important role played by local (often poorly characterised) Archaen and Proterozoic basement blocks as sand sources and drainage divides and, consequently, in controlling reservoir sandstone distribution in the region (Figure 8). Perhaps unsurprisingly, grains with an Archaean and Palaeoproterozoic signature (Pb Domain 1) are more abundant in basins further north, which is also consistent with provenance data from Triassic sandstones in the Faroe-Shetland region (Tyrrell et al., 2009 in press), but become increasingly less so in basins further south.

CONCLUSIONS:

1) The Pb isotopic composition of detrital K-feldspar offers a powerful method of determining the provenance of arkosic and sub-arkosic sandstones, and prospective source areas are also relatively easily characterised. When applied to Mesozoic sandstones in basins west of Ireland, the technique can place constraints on the scale and pattern of palaeodrainage and constrain the relative contribution of different source areas.

2) The bulk of K-feldspars in Permo-Triassic and Middle Jurassic sandstones from the eastern Rockall Basin (Dooish; 12/2-1z) appear to have been derived from three isotopically distinct source areas. Elements of the Lewisian Complex, similar to the Stanton Bank, formed an important and persistent source for all the sampled sandstones (Source 1), but other Lewisian Complex rocks (such as the Uist Block and its equivalents; Source 2) and a currently unidentified, likely Ketilidian, source (Source 3) variably provided additional sediment during deposition of the these sandstones. Intriguingly, Sources 2 and 3 do not appear to be available at the same time, which may suggest that the grains are being delivered through different tributary systems which are active at different times. There are very few

grains that could have been derived from southern sources, such as the Irish Massif and the Variscan Uplands. Although sources from the far north and west (e.g. SE Greenland) cannot be entirely ruled out, there are more proximal terranes that can supply feldspar with the requisite Pb isotopic composition. Similarly, it is difficult to clearly ascertain if grains were transported across the nascent Rockall Basin, although the overall textural immaturity of the sampled sandstones supports local sourcing. The simplest model for palaeodrainage, reconcilable with all the Pb data, suggests derivation directions from the north-west, north, north-east or directly from the eastern margin of the basin. North-derived dispersal directions appear to have persisted during deposition of the Permo-Triassic and the Middle Jurassic sequences, but more north-eastern and, potentially local, eastern sources appear to have supplied detritus intermittently.

3) There are difficulties constraining transport distances both during the Permo-Triassic and the Jurassic in the Dooish area, given the uncertainty associated with the nature and palaeo-position of all the potential sources, but palaeogeographic reconstructions suggest they are unlikely to be in excess of 300 km. It is probable that local sources (transport < 100 km) played an important role especially during the Jurassic. The Irish Massif appears to have acted consistently as a significant and persistent drainage divide or barrier during the Permo-Triassic and into the Late Jurassic. Although this massif prevented the transport of Variscan sand grains into the basins west of Ireland, it does not appear to have supplied significant sediment itself.

4) Determining the provenance of sandstones provides a first-order control on the distribution of reservoir intervals. The directions of sediment transport derived from the provenance data suggest more distal equivalents of the sedimentary rocks in 12/2-1z may have been deposited to the south and south-west, implying sandstones with similar bulk characteristics may occur at depth within the Rockall Basin.

5) The overall dispersal pattern of K-feldspar into basins west of Ireland during the Mesozoic suggests that Archaean and Proterozoic basement blocks played a crucial role in controlling drainage during this

prolonged period. It is therefore important to understand the nature, palaeo-position and late uplift history of these crustal blocks.

REFERENCES:

Audley-Charles, M.G. 1970. Triassic palaeogeography of the British Isles. *Quarterly Journal of the Geological Society, London,* **126**, 49-89.

Butterworth, P., Holba, A., Hertig, S., Hughes, W. & Atkinson, C. 1999. Jurassic non-marine source rocks and oils of the Porcupine Basin and other North Atlantic margin basins. *In:* Fleet, A.J. & Boldy, S.A.R. (eds.) *Petroleum Geology of Northwest Europe: Proceedings of the 5th Conference.* Geological Society, London, 471–486.

Cawood, P.A., Nemchin, A.A., Strachan, R.A., Kinny, P.D., Loewy, S. 2004. Laurentian provenance and an intracratonic tectonic setting for the Moine Supergroup, Scotland, constrained by detrital zircons from the Loch Eil and Glen Urquhart successions. *Journal of the Geological Society, London,* **161**, 861-874.

Connelly, J.N. & Thrane, K. 2005. Rapid determination of Pb isotopes to define Precambrian allochthonous domains: An example from West Greenland. *Geology*, **33**, 953–956.

21

Croker, P.F.& Shannon, P.M. 1987.The evolution and hydrocarbon prospectivity of the Porcupine Basin, Offshore Ireland. In: Brooks, J. & Glennie, K.W. (eds.) *Petroleum Geology of North West Europe.* Graham and Trotman, London, 633–642.

Clift, P.D., Shimizu, N., Layne, G.D. & Blusztajn, J. 2001. Tracing patterns of erosion and drainage in the Paleogene Himalaya through ion probe Pb isotope analysis of detrital K-feldspars in the Indus Molasse, India. *Earth and Planetary Science Letters*, **188**, 475-491.

Clift, P.D., Van Long, H., Hinton, R., Ellam, R.M., Hannigan, R., Tan, M.T., Blusztajn, J. & Duc, N.A. 2008. Evolving east Asian river systems reconstructed by trace element and Pb and Nd isotope variations in modern and ancient Red River-Song Hong sediments. *Geochemistry Geophysics Geosystems,* **9**, Q04039.

Dancer, P.N., Kenyon-Roberts, S.M., Downey, J.W., Baillie, J.M., Meadows, N.S. & Maguire, K. 2005. The Corrib gas field, offshore west of Ireland. *In*: Doré, A.G. & Vining, B.A. (eds.) *Petroleum Geology: North-West Europe and Global Perspectives – Proceedings to the 6th Petroleum Geology Conference*. Geological Society, London, 1035-1046.

DeWolf, C.P. & Mezger, K., 1994. Lead isotope analyses of leached feldspars: Contraints on the early crustal history of the Grenville Orogen. *Geochemica et Cosmochemica Acta,* **58**, 5537-5550.

Eide, E.A. 2002. *BATLAS – Mid Norway plate reconstruction atlas with global and North Atlantic perspectives*. Geological Survey of Norway.

Geraghty, D. 1999. Petrography and possible provenance of Jurassic reservoirs in the Porcupine Basin. *Abstracts to the 43rd Irish Geological Research Meeting: Irish Journal of Earth Sciences,* **17**, 130.

Haughton, P., Praeg, D., Shannon, P., Harrington, G., Higgs, K., Amy, L., Tyrrell, S., & Morrissey, T., 2005. First results from shallow stratigraphic boreholes on the eastern flank of the Rockall Basin, offshore western Ireland. *In:* Doré, A.G. & Vining, B.A. (eds.) *Petroleum Geology: North-West Europe and Global Perspectives – Proceedings to the 6th Petroleum Geology Conference.* Geological Society, London, 1077–1094.

Hemming, S.R., Broecker, W.S., Sharp, W.D., Bond, G.C., Gwiazda, R.H., McManus, J.F., Klas, M., & Hajdas, I. 1998. Provenance of Heinrich layers in core V28-82, northeastern Atlantic: $^{40}Ar/^{39}Ar$ ages of ice-rafted hornblende, Pb isotopes in feldspar grains, and Nd-Sr-Pb isotopes in the fine sediment fraction. *Earth and Planetary Science Letters*, **164**, 317-333.

Moore, T.E., Hemming, S.R., & Sharp, W.D. 1997. Provenance of the Carboniferous Nuka Formation, Brooks Range Alaska: a multicomponent isotope provenance study with implications for age of cryptic crystalline basement. *In:* Dumoulin, J.A. & Gray, J.E. (eds.) *Geologic Studies in Alaska by the U.S Geological Survey, 1995.* U.S. Geological Survey, Professional Paper, **1574**, 173-194.

Morton, A.C., Herries, R. & Fanning, C.M. 2007. Correlation of Triassic sandstones in the Strathmore Field, west of Shetland, using heavy mineral provenance signatures. *In:* Mange, M. & Wright, D.K. (eds.) *Heavy Minerals In Use*. Developments in Sedimentology, **58**, 1037-1072.

Naylor, D., & Shannon, P.M. 2005. The structural framework of the Irish Atlantic Margin. In: Doré, A.G. & Vining, B.A. (eds.) *Petroleum Geology: North-West Europe and Global Perspectives – Proceedings to the 6th Petroleum Geology Conference*. Geological Society, London, 1009–1021.

Praeg, D. 2004. Diachronous Variscan late-orogenic collapse as a response to multiple detachments: a view from the internides in France to the foreland in the Irish Sea. *In:* Wilson, M., Neumann, E.-R., Davies, G.R., Timmerman, M.J., Heeremans, M. & Larsen, B.T. (eds) *Permo-Carboniferous Magmatism and Rifting in Europe.* Geological Society, London, Special Publications, **223**, 89-138.

Robinson, A.J. & Canham, A.C., 2001. Reservoir characteristics of the Upper Jurassic sequence in the 35/8-2 discovery, Porcupine Basin. *In:* Shannon, P.M., Haughton, P.D.W. & Corcoran, D.V. (eds) *The Petroleum Exploration of Ireland's offshore Basins.* Geological Society, London, Special Publications, **188**, 301-321.

Scotese, C.R. 2002. http://www.scotese.com, (PALEOMAP website).

Tate, M.P., Dodd, C.D. & Grant, N.T. 1999. The Northeast Rockall Basin and its significance in the evolution of the Rockall-Faeroes/East Greenland rift system. In: Fleet, A.J. & Boldy, S.A.R. (eds.) *Petroleum Geology of Northwest Europe: Proceedings of the 5th Conference.* Geological Society, London, 391–406.

Torsvik, T.H., Van der Voo, R., Meert, J.G., Mosar, J. & Walderhaug, H.J. 2001. Reconstructions of the continents around the north Atlantic at about the 60th parallel. *Earth and Planetary Science Letters,* **197**, 55–69.

Tyrrell. S., Haughton, P.D.W., Daly, J.S., Kokfelt, T.F. & Gagnevin, D. 2006. The use of the common Pb isotope composition of detrital K-feldspar grains as a provenance tool and its application to Upper Carboniferous palaeodrainage, Northern England. *Journal of Sedimentary Research,* **76**, 324-345.

Tyrrell, S., Haughton, P.D.W. & Daly J.S. 2007. Drainage re-organization during break-up of Pangea revealed by *in-situ* Pb isotopic analysis of detrital K-feldspar. *Geology,* **35**, 971-974.

Tyrrell, S., Leleu, S., Souders, A.K., Haughton, P.D.W. & Daly, J.S. 2009. K-feldspar sand-grain provenance in the Triassic, west of Shetland: a first-cycle sedimentary fingerprint? *Geological Journal,* **44***,* 692-710.

Vitrac, A.M., Albarede, F. & Allégre, C.J., 1981. Lead isotopic composition of Hercynian granite K-feldspars constrains continental genesis. *Nature*, **291**, 460-464.

Walsh, A., Knag, G., Morris, M., Quinquis, H., Tricker, P., Bird, C., & Bower, S., 1999. Petroleum geology of the Irish Rockall Trough. *In:* Fleet, A.J. and Boldy, S.A.R. (eds.) *Petroleum Geology of Northwest Europe: Proceedings of the 5th Conference.* Geological Society, London, 433–444.

Warrington, G., Audley-Charles, M.G., Elliot, R.E., Evans, W.B., Ivimey-Cook, H.C., Kent, P.E., Robinson, P.L., Shotton, F.W. & Taylor, .FM. 1980. A correlation of Triassic rocks in the British Isles. *Special Reports of the Geological Society of London,* **13.**

Warrington, G. & Ivimey-Cooke, H.C. 1992. Triassic. *In:* Cope, J.C.W., Ingham, J.K. & Rawson, P.F. (eds.) *Atlas of Palaeogeography and Lithofacies.* Geological Society, London, Memoir, **13,** 97-106.

Williams, B.P.J., Shannon, P.M., & Sinclair, I.K., 1999, Comparative Jurassic and Cretaceous tectono-stratigraphy and reservoir development in the Jeanne d'Arc and Porcupine basins. *In:* Fleet, A.J. and Boldy, S.A.R. (eds.), *Petroleum Geology of Northwest Europe: Proceedings to the 5th Petroleum Geology Conference*. Geological Society, London, 487–499.

Ziegler, P.A. 1991. *Geological Atlas of Western and Central Europe*. Geological Society Publishing House. Shell International Petroleum Maatschappij B.V.

Figure captions:

Fig. 1. Maps illustrating A) the basins offshore western Ireland, showing the position of Dooish well 12/2-1z and other regional wells from which K-feldspar provenance data has been retrieved; and B) the broader North Atlantic region showing the distribution of Pb domains (adapted from Tyrrell *et al*., 2007) with a plot showing Pb isotopic composition of these domains. Also shown are the approximate location of the geoseimic section in Figure 2 and the position of hydrocarbon fields and discoveries referred to in text. CG = Corrib gasfield; CO = Connemara oil accumulation; DG = Dooish gas condensate discovery; SP = Spanish Point gas condensate discovery; SF = Strathmore field.

Fig. 2. Representative NW-SE geoseismic section through the NE Rockall Basin margin illustrating the pre-Cretaceous tilted fault block structure of the Dooish trend, offset to the south of well 12/2-1z. Figure is reproduced courtesy of the Petroleum Affairs Division (Ireland) and PGS Geophysical.

Fig. 3. Simplified gamma and sonic log wireline profiles from well 12/2-1z, illustrating the stratigraphy and contrasting response between the A, B and C sandstones (left) with $^{206}Pb/^{204}Pb$ - $^{207}Pb/^{204}Pb$ lead space plots showing the variation of Pb K-feldspar populations with stratigraphy.

Fig. 4. Sedimentological logs of cores 1 to 3 in well 12/2-1z, illustrating the character and distribution of facies. Samples from which the Pb composition of K-feldspar have been analysed are highlighted with a red circle.

Fig. 5. Photomicrographs (XPL and PPL) of (**a**) A sandstones with typical bimodal grain distribution of rounded and finer, angular grains; (**b**) arkosic, lithic, B sandstones; (**c**) C sandstones with bimodal grain size distribution; (**d**) perthitic microcline K-feldspar grains from A sandstones; (**e**) quartzo-feldspathic gneissic lithic from B sandstones and (**f**) fine grained calcareous sandstones associated with soil forming processes from upper B sandstones.

Fig. 6. $^{206}Pb/^{204}Pb$ - $^{207}Pb/^{204}Pb$ lead space plots for all the Dooish sandstones K-feldspar. Data are plotted with reference to Pb domains 1-4 (after Tyrrell *et al.* 2007, Figure 1B). Three groupings, corresponding to source 1, 2 and 3, are highlighted.

Fig. 7. $^{206}Pb/^{204}Pb$ - $^{207}Pb/^{204}Pb$ lead space plots for the 3 sources, plotted with Pb data from (**a**) the Nagssugtoqidian Mobile Belt of SE Greenland; (**c**) Lewisian Complex Rocks from NW Scotland; (**c**) offshore crystalline basement blocks from the NW Atlantic and (**d**) crystalline basement from onshore western Ireland. Pb basement data from Tyrrell *et al.* 2007 (Figure 1B) and references therein.

Fig. 8. Palaeogeographic reconstructions of the circum North Atlantic region during the Late Permian – Early Triassic and Middle Jurassic (after Scotese 2002; Eide *et al.* 2002; Torsvik *et al.* 2001; Zeigler

1999; Williams *et al.* 1999), showing the palaeodrainage directions (arrows) during the deposition of the

Dooish sandstones. The land-masses are colour coded so as to reflect their bulk Pb signature (Tyrrell

et al. 2007) with darker colours used to highlight areas that are potential sources. Also shown, for

reference) are the orientation of drainage axes supplying the Corrib Gasfield sandstones (Lower

Triassic, Slyne Basin) and Upper Jurassic of the northern Porcupine Basin (from Tyrrell *et al.* 2007).

ADL = Anton Dohrn Lineament; CM = Cornubia Massif; EISB = East Irish Sea Basin; FC = Flemish

Cap; GB = Galicia Bank; HP = Hebridean Platform; IM = Irish Massif; LH = Labadie Bank High; LB =

London-Bradbant Massif; PB = Porcupine Bank; PH = Porcupine High; RB = Rockall Bank; SP =

Shetland Platform; WM = Welsh Massif.

Fig. 9. ^{206}Pb/^{204}Pb - ^{207}Pb/^{204}Pb lead space plots for (**a**) Dooish K-feldspars compared to populations

from Triassic sandstones in the Slyne Basin, including those from the Corrib Gasfield; (**b**) Dooish K-

feldspars compared to populations from Upper Jurassic sandstones in the Northern Porcupine Basin

(the Connemara field and the Spanish Point Gas Condensate); and (**c**) Dooish K-feldspars compared

with populations from Cretaceous sandstones from shallow boreholes on the eastern Rockall Basin

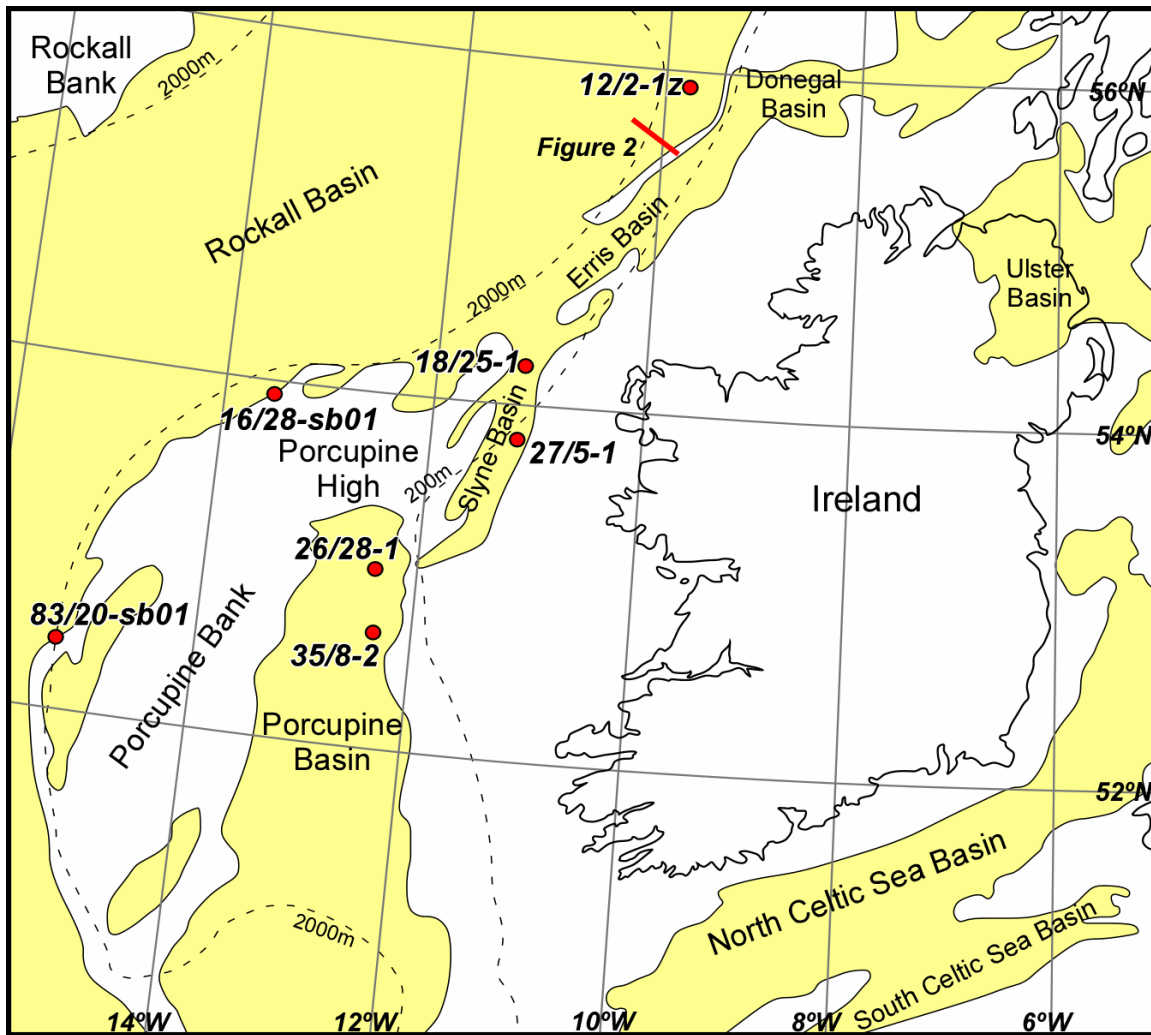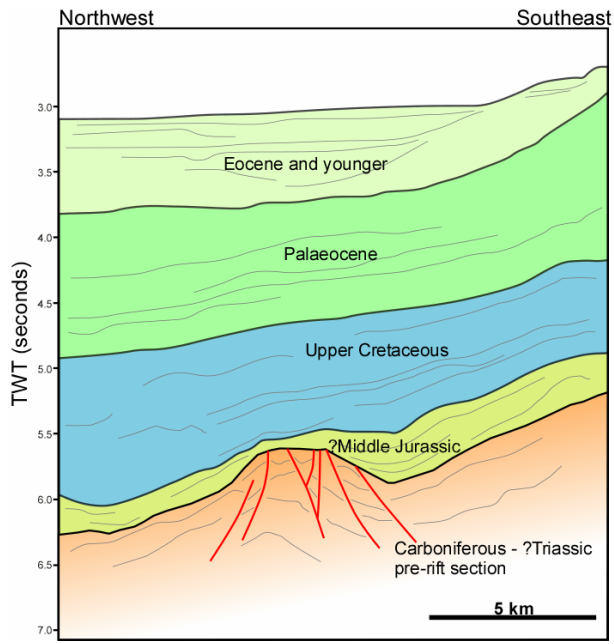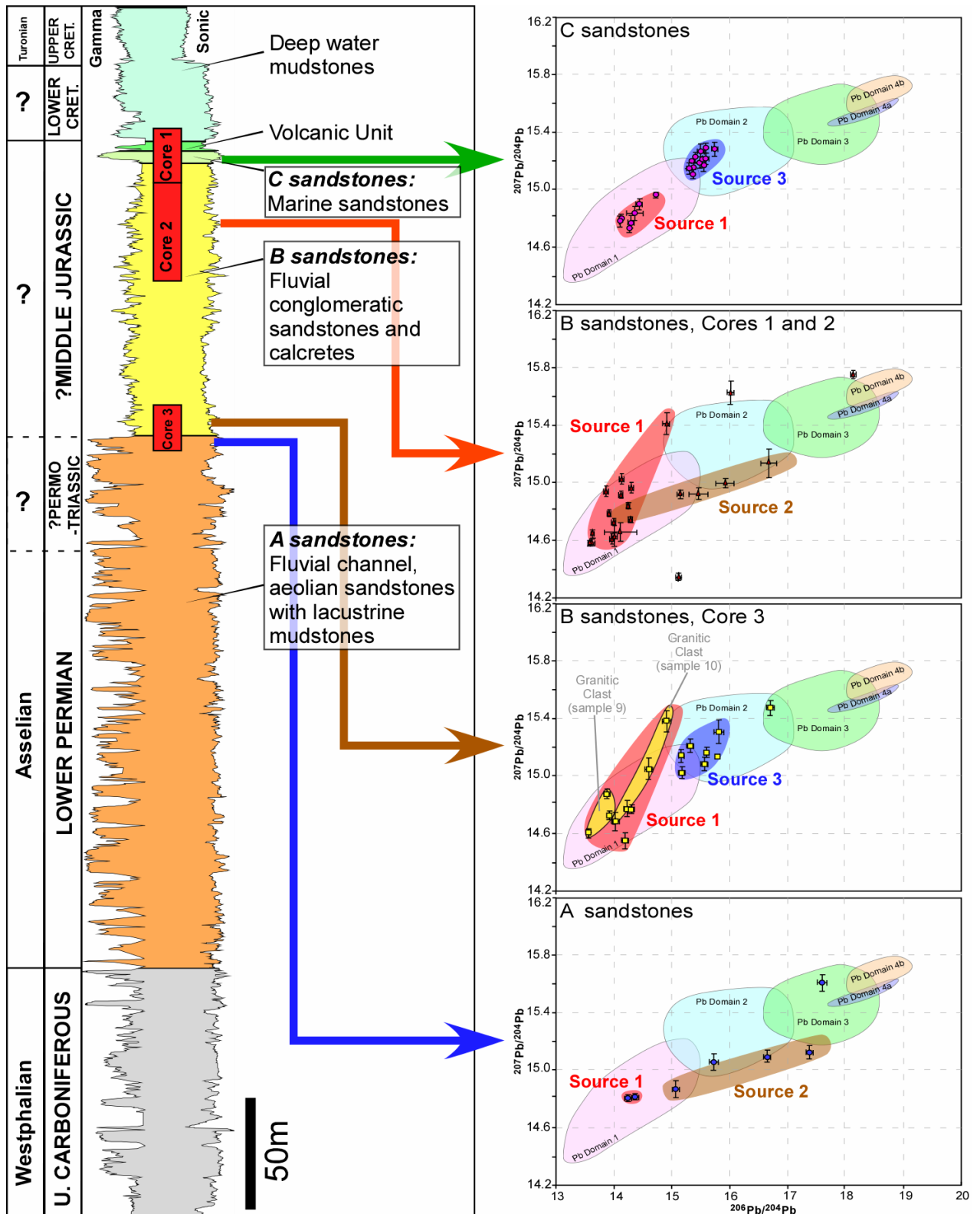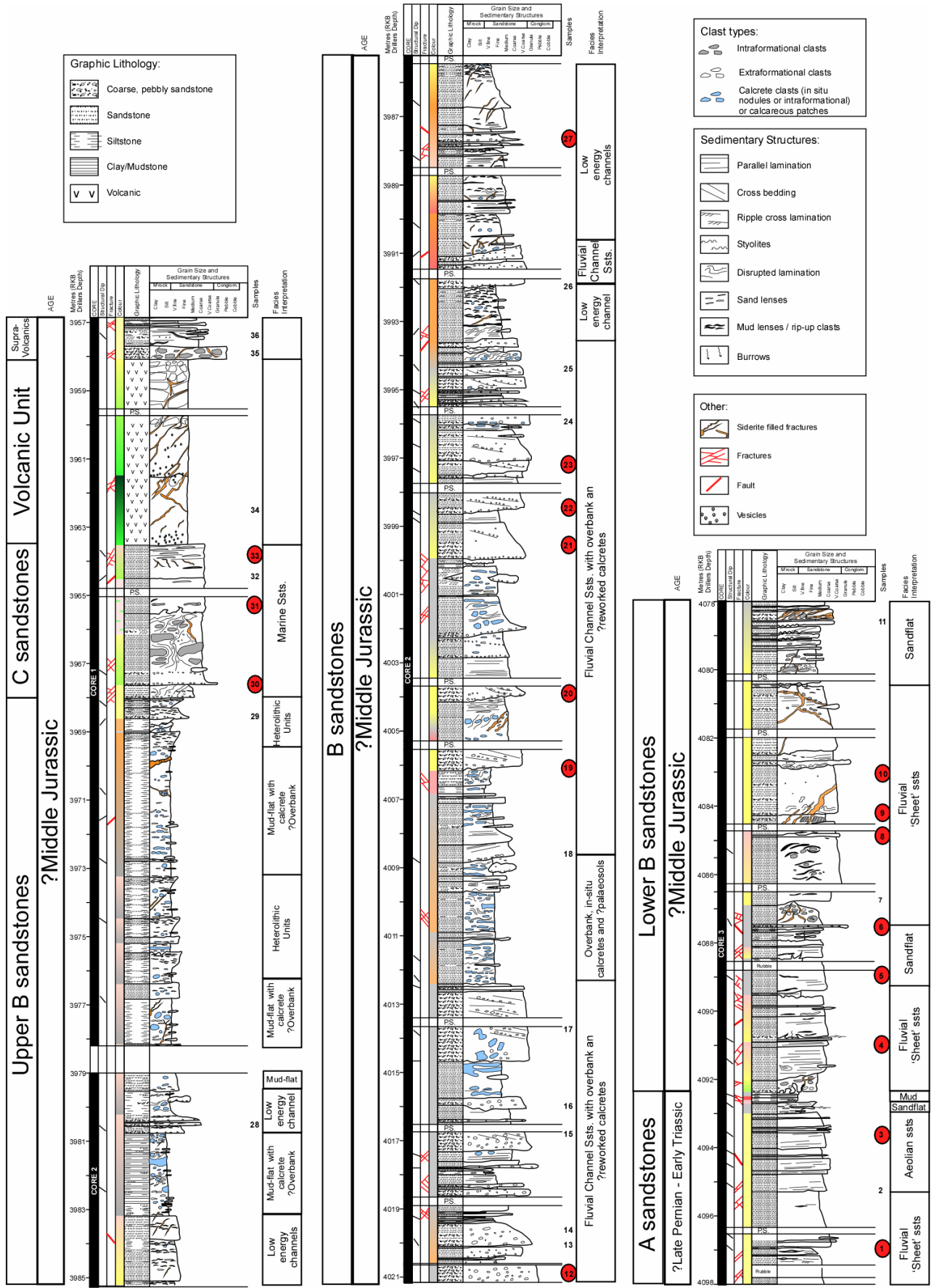margin. Previously published data is from Tyrrell *et al.* 2007.

Figure 1

Figure 2

Figure 3

Figure 4

Figure 5

Figure 6

Tyrrell et al.

Palaeodrainage in the Rockall Basin

Figure 7

34
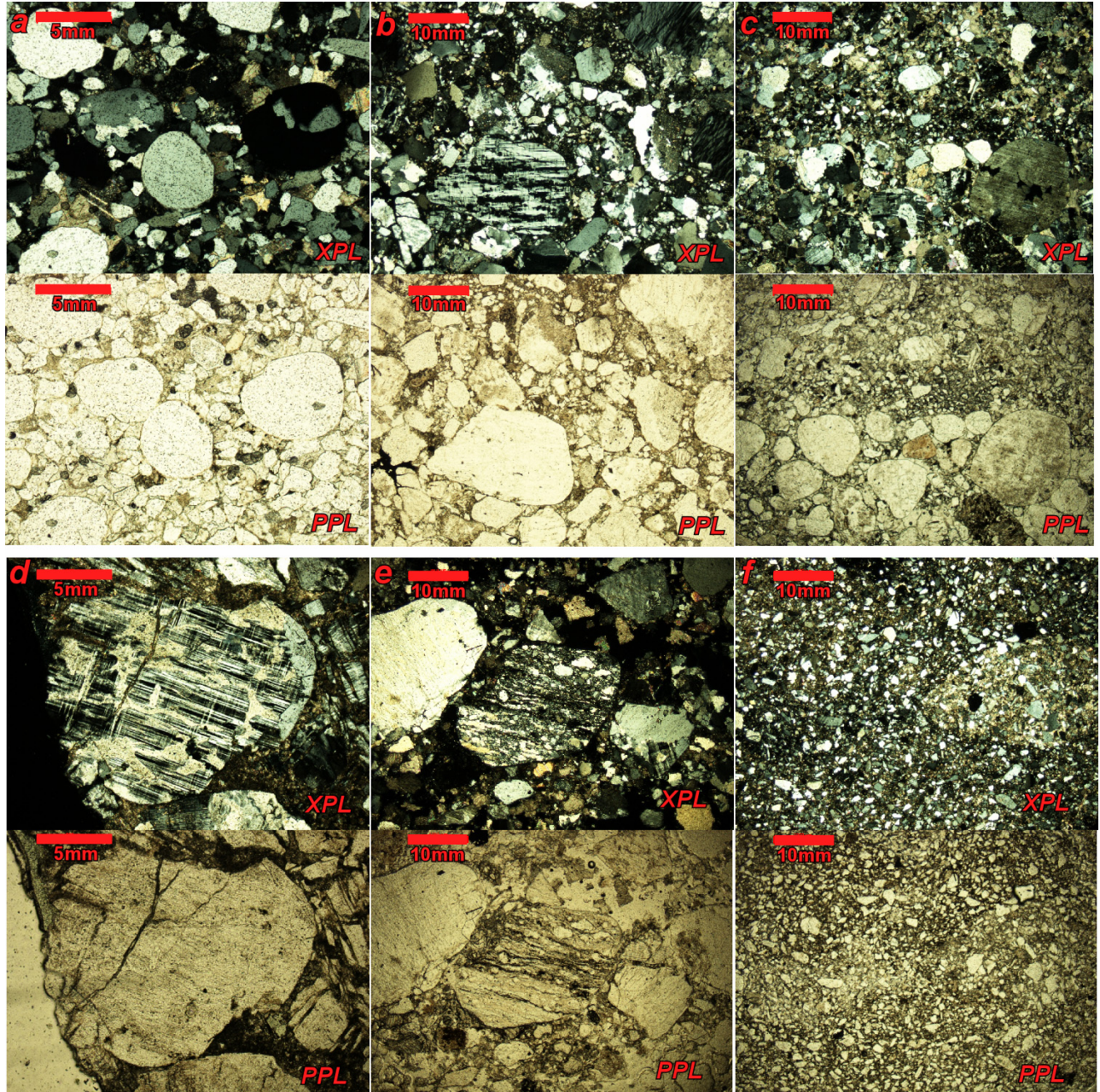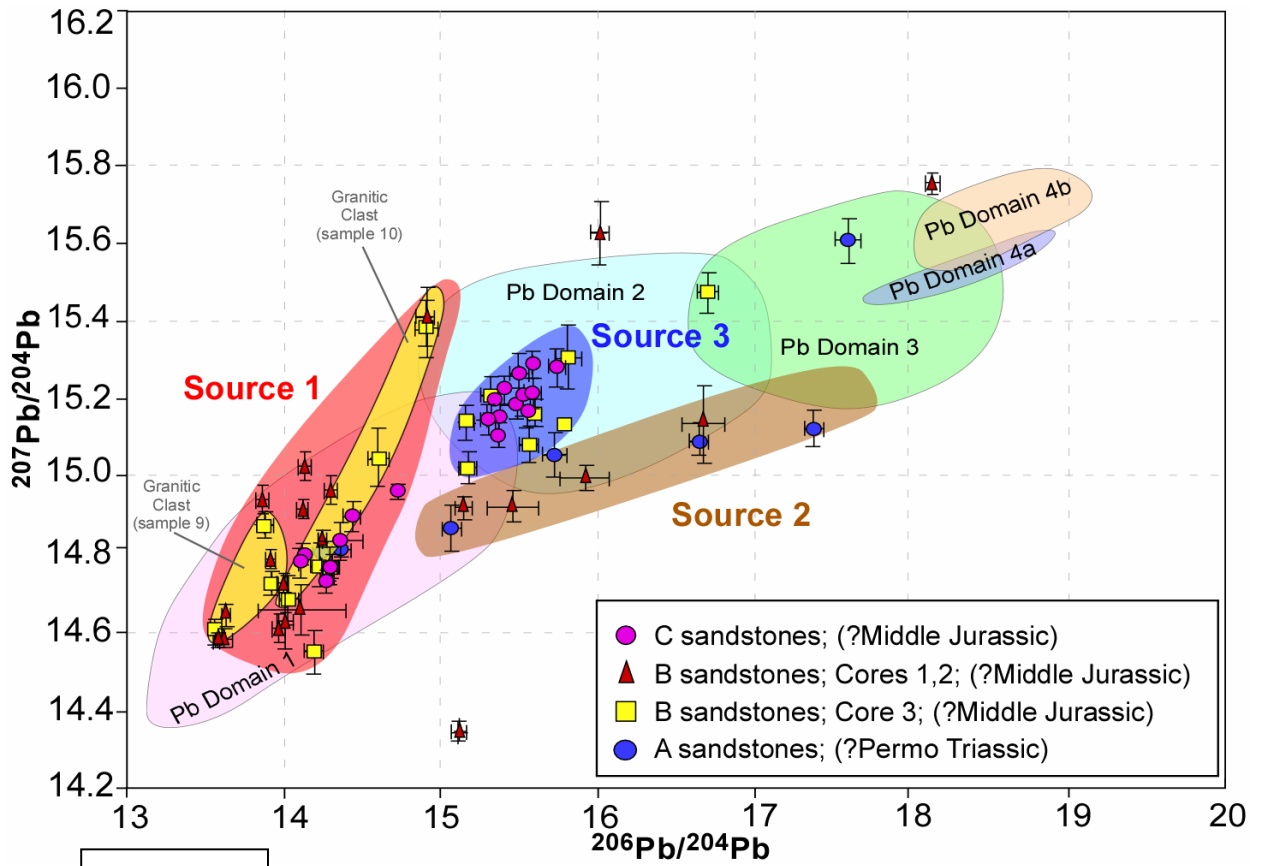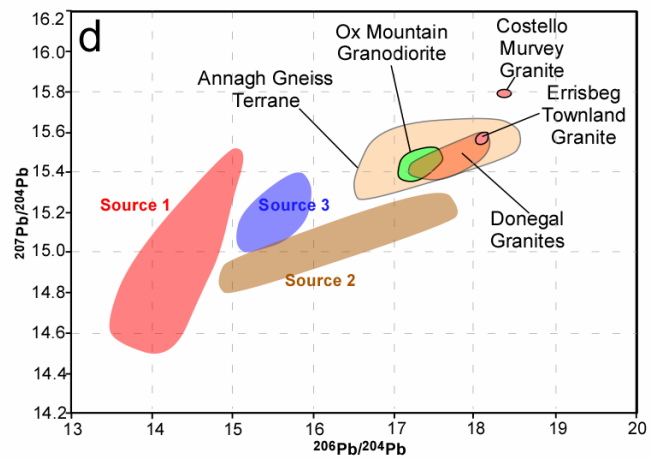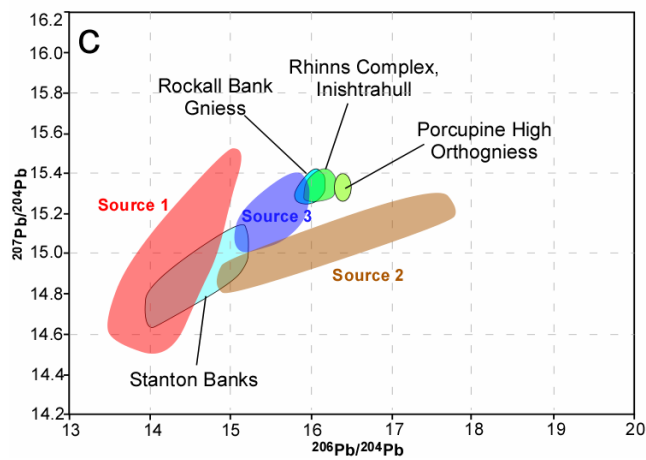
Figure 8

Figure 9

Table 1: Pb concentration, Pb isotopic and bulk feldspar composition data of detrital K-feldspars from sandstones in the Dooish well (12/2-1z). Data have been collected using two techniques (F = Faraday collector configuration, IC = ion counter collector configuration), detailed in the text.

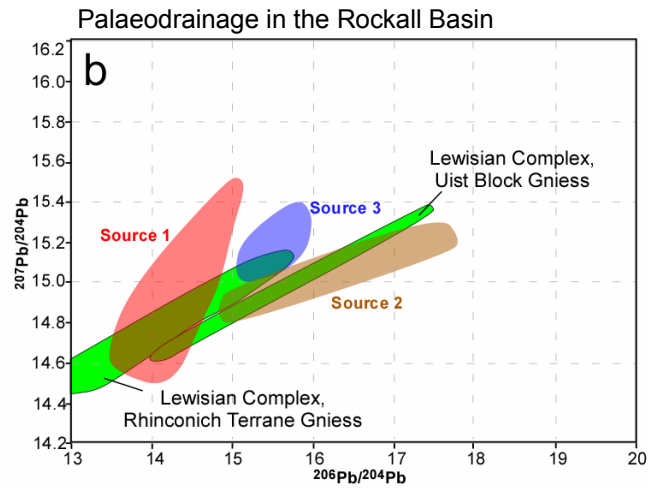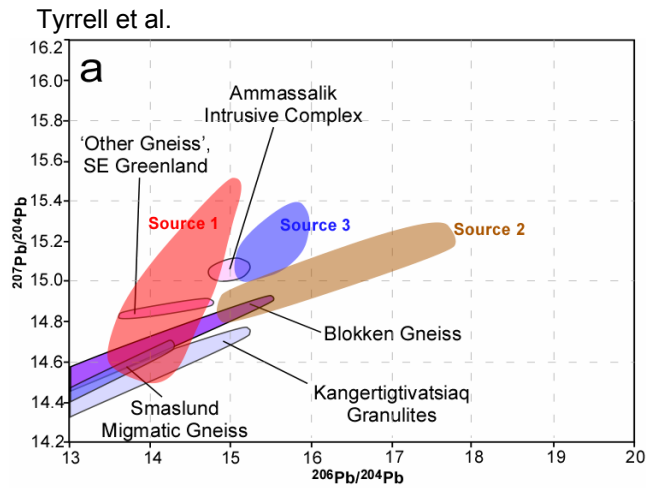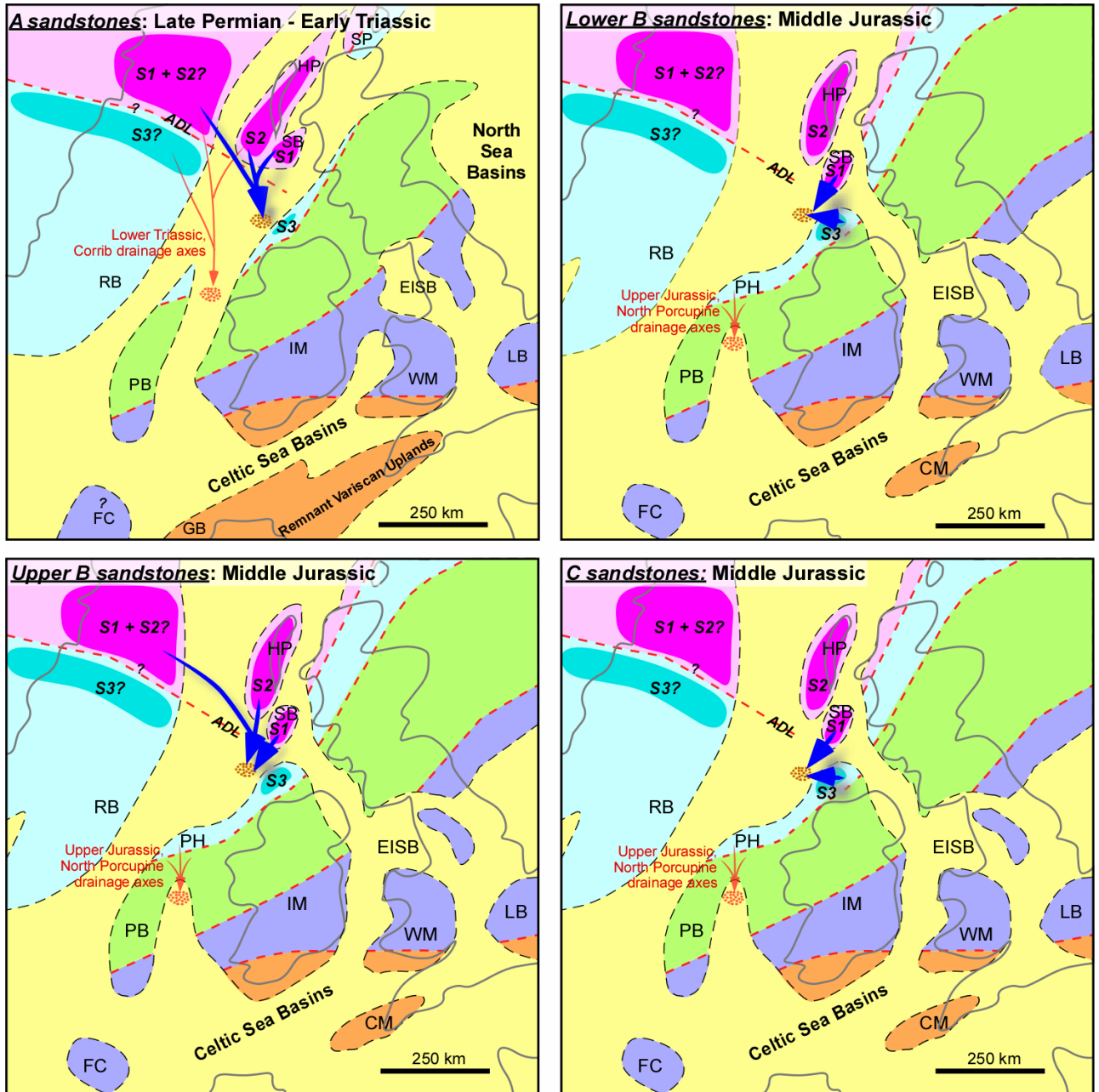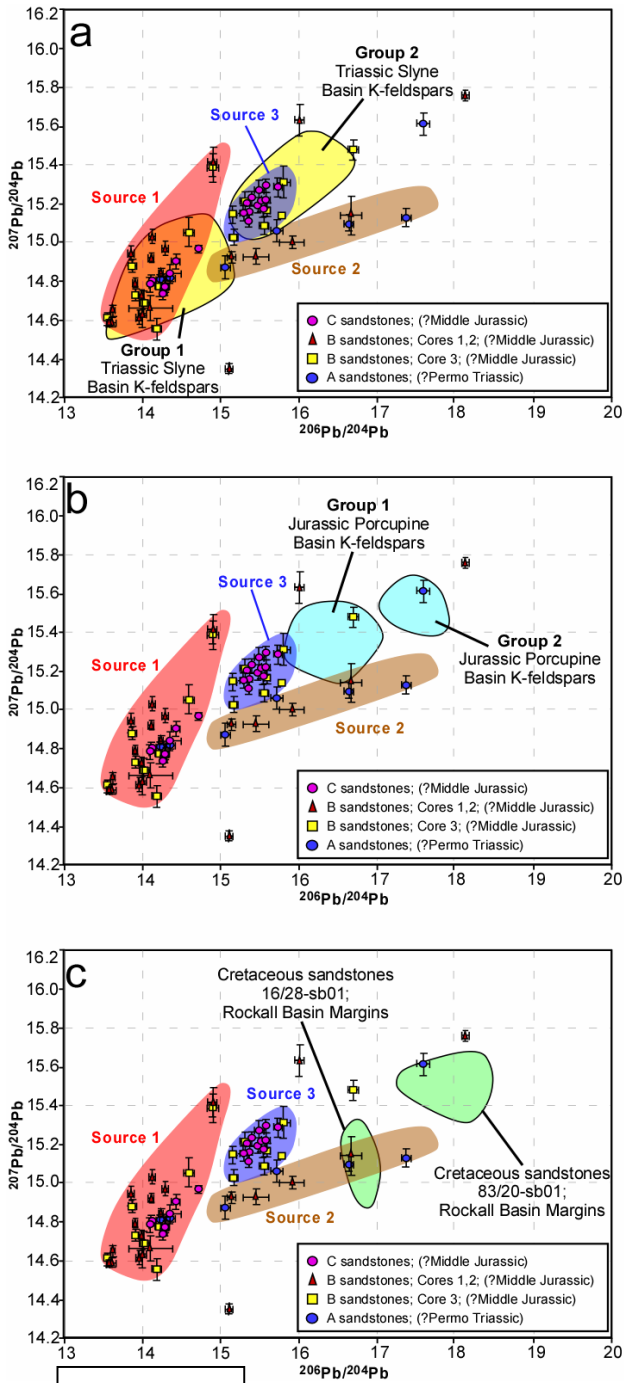| Sample	Technique	Depth (m)	Grain	Or : Ab : An	Package	Pb (ppm)	$^{206}Pb/^{204}Pb$	2σ	$^{207}Pb/^{204}Pb$	2σ	$^{208}Pb/^{204}Pb$	2σ
1	F	4096.90	6	97.15 : 2.58 : 0.26	A	-	15.077	0.063	14.867	0.059	34.303	0.137
	F	4096.90	8	96.53 : 3.36 : 0.11	A	-	14.252	0.052	14.813	0.051	34.387	0.122
3	IC	4093.55	1	97.55 : 2.43 : 0.02	A	5	14.344	0.039	14.806	0.031	34.255	0.153
	IC	4093.55	2	97.00 : 3.00 : 0	A	7	17.360	0.062	15.116	0.043	37.214	0.257
	IC	4093.55	3	97.05 : 2.95 : 0	A	19	17.576	0.084	15.605	0.060	38.046	0.353
	IC	4093.55	5	98.31 : 1.69 : 0	A	12	16.632	0.057	15.084	0.041	36.520	0.235
	IC	4093.55	7	97.69 : 2.28 : 0.03	A	10	15.710	0.076	15.055	0.058	35.417	0.313
4	IC	4091.00	1	98.34 : 1.64 : 0.03	B1	34	14.598	0.029	15.042	0.029	34.839	0.162
	IC	4091.00	2	96.23 : 3.77 : 0	B1	11	15.314	0.048	15.203	0.047	34.981	0.250
	IC	4091.00	4	97.41 : 2.59 : 0	B1	9	15.816	0.083	15.301	0.081	35.442	0.408
	IC	4091.00	5	96.85 : 3.15 : 0	B1	8	14.197	0.057	14.540	0.057	33.653	0.297
	IC	4091.00	6	97.88 : 2.06 : 0.6	B1	17	15.163	0.042	15.132	0.043	34.880	0.228
5	F	4089.00	2	95.19 : 4.81 : 0	B1	-	14.308	0.030	14.760	0.032	34.079	0.072
6	IC	4087.50	2	87.76 : 11.91 : 0.33	B1	25	15.575	0.059	15.073	0.048	34.896	0.277
	IC	4087.50	3	83.38 : 15.18 : 1.45	B1	16	16.708	0.069	15.467	0.053	35.534	0.300
	IC	4087.50	5	96.15 : 3.85 : 0	B1	11	15.175	0.051	15.014	0.041	34.550	0.241
8	F	4084.85	1	90.85 : 9.15 : 0	B1	-	15.582	0.036	15.161	0.034	34.980	0.080
9*	IC	4084.00	2	96.44 : 3.02 : 0.54	B1	24	13.876	0.029	14.867	0.033	36.160	0.203
	IC	4084.00	3	94.63 : 5.37 : 0	B1	13	13.566	0.029	14.592	0.033	35.375	0.206
	IC	4084.00	4	95.34 : 4.64 : 0.02	B1	8	13.927	0.030	14.718	0.032	35.858	0.211
10*	IC	4083.10	1	96.21 : 3.79 : 0	B1	9	14.598	0.071	15.044	0.075	35.242	0.403
	IC	4083.10	2	95.82 : 4.18 : 0	B1	22	14.230	0.055	14.764	0.058	34.653	0.319
	IC	4083.10	3	96.91 : 3.09 : 0	B1	10	14.909	0.072	15.373	0.074	36.263	0.408
	IC	4083.10	4	96.04 : 3.06 : 0	B1	36	14.028	0.057	14.672	0.061	34.127	0.331
12	F	4021.10	1	97.81 : 2.19 : 0	B2	-	14.236	0.086	13.903	0.060	32.142	0.161
	F	4021.10	6	96.44 : 3.50 : 0.05	B2	-	13.536	0.088	13.020	0.096	30.252	0.211
19	F	4006.00	1	97.03 : 2.97 : 0	B2	-	15.159	0.052	14.920	0.029	34.562	0.080
	F	4006.00	2a	96.40 : 3.60 : 0	B2	-	15.463	0.164	14.924	0.040	34.672	0.160
	F	4006.00	2b	96.40 : 3.60 : 0	B2	-	15.929	0.158	14.998	0.033	35.006	0.142
20	IC	4004.00	2	97.01 : 2.99 : 0	B2		14.140	0.043	15.026	0.036	35.102	0.274
	IC	4004.00	3	-	B2		13.871	0.042	14.942	0.036	34.568	0.265
	IC	4004.00	5	97.33 : 2.67 : 0	B2		13.977	0.042	14.611	0.035	33.878	0.264
	IC	4004.00	6	97.24 : 2.72 : 0.04	B2		14.306	0.043	14.969	0.036	34.600	0.267
21	IC	3999.70	1	97.38 : 2.62 : 0	B2		15.111	0.036	14.347	0.024	33.744	0.095
	IC	3999.70	2	96.06 : 3.94 : 0	B2		14.003	0.033	14.726	0.024	34.806	0.096
	IC	3999.70	3	97.47 : 2.51 : 0.02	B2		14.296	0.034	14.744	0.024	35.295	0.104
	IC	3999.70	4	97.64 : 2.36 : 0	B2		18.142	0.046	15.755	0.027	35.426	0.112
	IC	3999.70	5	96.23 : 3.77 : 0	B2		13.923	0.033	14.792	0.024	34.287	0.098
	IC	3999.70	6	97.36 : 2.64 : 0	B2		14.127	0.034	14.917	0.024	34.677	0.094
22	IC	3998.50	1	97.53 : 2.47 : 0	B2		16.018	0.063	15.627	0.079	35.728	0.323
	IC	3998.50	2	97.21 : 2.79 : 0	B2		14.018	0.055	14.630	0.074	33.986	0.297
	IC	3998.50	3	93.75 : 6.25 : 0	B2		14.900	0.059	15.412	0.078	36.387	0.322
23	F	3997.25	6	-	B2	-	14.254	0.027	14.840	0.018	34.465	0.044
	F	3997.25	3a	-	B2	-	13.581	0.019	14.578	0.019	33.818	0.046
	F	3997.25	3b	-	B2	-	13.626	0.052	14.585	0.023	33.811	0.066
27	F	3987.60	1	96.96 : 3.04 : 0	B2	-	16.683	0.131	15.137	0.100	35.670	0.248
	F	3987.60	5a	95.30 : 4.68 : 0.02	B2	-	14.122	0.282	14.656	0.065	34.406	0.222
	F	3987.60	5b	95.30 : 4.68 : 0.02	B2	-	13.645	0.030	14.645	0.029	34.163	0.072
30	F	3967.65	1	96.03 : 3.97 : 0	C	-	14.295	0.041	14.780	0.044	34.412	0.103
	F	3967.65	6	97.19 : 2.77 : 0.05	C	-	14.376	0.140	14.839	0.046	34.636	0.153
	F	3967.65	7	96.20 : 3.76 : 0.04	C	-	14.734	0.019	14.966	0.020	34.588	0.047
31	IC	3965.25	1	-	C	38	15.353	0.031	15.193	0.028	34.963	0.154
	IC	3965.25	2	-	C	46	15.527	0.031	15.204	0.028	35.371	0.152
	IC	3965.25	3	-	C	13	15.387	0.031	15.156	0.028	35.160	0.153
	IC	3965.25	4	-	C	25	14.290	0.031	14.733	0.030	34.156	0.161
	IC	3965.25	5	-	C	27	14.132	0.028	14.805	0.027	34.553	0.150
	IC	3965.25	6	-	C	3	15.496	0.031	15.182	0.027	35.187	0.149
	IC	3965.25	7	-	C	36	15.380	0.034	15.110	0.031	34.863	0.166
	IC	3965.25	8	-	C	11	15.593	0.036	15.292	0.034	35.350	0.181
33	IC	3963.83	1	-	C	41	14.443	0.042	14.904	0.041	34.765	0.197
	IC	3963.83	2	-	C	5	15.307	0.041	15.151	0.038	35.067	0.186
	IC	3963.83	3	-	C	38	14.121	0.037	14.783	0.036	34.484	0.174
	IC	3963.83	4	-	C	48	15.594	0.043	15.220	0.040	35.175	0.193
	IC	3963.83	5	-	C	51	15.412	0.040	15.227	0.036	35.219	0.175
	IC	3963.83	6	-	C	39	15.548	0.042	15.167	0.038	35.122	0.185
	IC	3963.83	7	-	C	14	15.509	0.058	15.265	0.056	34.956	0.265
	IC	3963.83	8	-	C	6	15.746	0.050	15.285	0.047	35.121	0.236

* Analysis of K-feldspar crystals in granitic clasts